THE JOURNAL OF BIOLOGICAL CHEMISTRY VOL. 280, NO. 48, pp. 40282–40292, December 2, 2005

HDAC6 and Microtubules Are Required for Autophagic Degradation of Aggregated Huntingtin*[S]

Received for publication, August 9, 2005, and in revised form, September 19, 2005 Published, JBC Papers in Press, September 28, 2005, DOI 10.1074/jbc.M508786200

Atsushi Iwata, Brigit E. Riley, Jennifer A. Johnston[1], and Ron R. Kopito[2]

From the Department of Biological Sciences, BIO-X Program, Stanford University, Stanford, California 94305-5430

CNS neurons are endowed with the ability to recover from cytotoxic insults associated with the accumulation of proteinaceous polyglutamine aggregates via a process that appears to involve capture and degradation of aggregates by autophagy. The ubiquitin-proteasome system protects cells against proteotoxicity by degrading soluble monomeric misfolded aggregation-prone proteins but is ineffective against, and impaired by, non-native protein oligomers. Here we show that autophagy is induced in response to impaired ubiquitin proteasome system activity. We show that ATG proteins, molecular determinants of autophagic vacuole formation, and lysosomes are recruited to pericentriolar cytoplasmic inclusion bodies by a process requiring an intact microtubule cytoskeleton and the cytoplasmic deacetylase HDAC6. These data suggest that HDAC6-dependent retrograde transport on microtubules is used by cells to increase the efficiency and selectivity of autophagic degradation.

Accumulation of protein aggregates within intracellular inclusion bodies (IB)[3] is a pathological hallmark of most neurodegenerative diseases. In Huntington disease (HD) and related dominantly inherited, late-onset neurodegenerative diseases, pathology is the direct consequence of expansion of CAG triplet repeats that encode homopolymeric tracts of glutamine (polyQ) within the mutant gene product (1). In HD, these polyQ tracts typically consist of greater than 39 glutamines in the huntingtin protein (Htt), while Htt with fewer than ~30 glutamines is not associated with disease (2). This CAG length dependence of disease onset and severity in HD and in related CAG expansion disorders (1) correlates strongly with the propensity of expanded polyQ proteins to aggregate *in vitro*, in cell culture (3). or in mouse (4). or *Drosophila* (5) models of HD. There is compelling data in support of the hypothesis that CAG expansion and other neurodegenerative diseases are disorders of protein conformation, in which normally well behaved proteins adopt non-native toxic oligomeric conformations (6–8). Aggregated forms of polyQ-expanded Htt can disrupt cellular function in a variety of ways including specific co-aggregation with and inactivation of nuclear transcription factors (9, 10), interference with axonal transport (11), damage to mitochondrial or cellular membranes (12), and impairment of the ubiquitin-proteasome system (13, 14). Recent studies have suggested that cellular toxicity (15, 16) and ubiquitin-proteasome system impairment (17) is associated with non-native soluble oligomeric or protofibrillar forms of aggregation-prone proteins such as Htt, whereas large, microscopically detectable, IB may be cytoprotective (18).

Because polyglutamine aggregates are largely insoluble, refractory to chemical denaturation (19), and because they accumulate in inclusion bodies (IB) (20), it is widely assumed that cells have little or no capacity to eliminate them. However, several recent studies have established that neurons in conditional transgenic mouse models of polyQ disease have the capacity to recover from the toxicity of transient expression of aggregation prone proteins containing expanded polyglutamine tracts (21, 22). Thus, cellular mechanisms must exist to suppress the toxicity associated with intracellular accumulation of conformationally defective mutant proteins like Htt and ataxin-1. Elucidating the molecular processes underlying these cytoprotective mechanisms is clearly important to the development of therapeutic approaches to the treatment of Huntington and other neurodegenerative diseases.

A growing body of evidence supports the hypothesis that autophagy is a primary mechanism through which mammalian cells can capture and degrade protein aggregates. In classic autophagy, cytoplasmic contents, including ribosomes, soluble proteins and organelles, are captured into bilamellar autophagosomes, which, upon fusion with lysosomes, mature into degradative autolysosomes (23). In yeast these events require the function of *ATG* genes, which encode proteins called Atgs (24, 25). A functional role for autophagy in clearance of aggregated Htt is suggested by the observation that 3-methyladenine, an inhibitor of type III phosphoinositide 3-kinases required for many vesicular trafficking events, including autophagosome formation (26), increases levels of polyQ-expanded Htt inclusions and decreases the clearance of aggregates from mammalian cells expressing these constructs (27, 28). Pharmacological activation of mTOR, a protein kinase that regulates a myriad of cellular responses to changes in nutrient and hormonal status, including autophagy (29), delays the neurotoxicity associated with mutant Htt in cellular (30) and animal (31) models of HD. Ultrastructural evidence suggesting a proliferation of lysosomes and autophagic bodies in striatal neurons expressing mutant Htt (32) and in Huntington (33) and Alzheimer disease brains (34), further supports a linkage between degeneration and autophagy (35), although these morphological studies cannot distinguish between a role for autophagy in cytoprotection or cell death. Recently, we reported that RNAi-mediated Atg knockdown leads to increased steady-state levels of Htt and completely prevents clearance of cytoplasmic polyglutamine aggregates from cell models of HD (36). We also observed that cytoplasmic IB are consistently labeled with antibodies to endogenous Atgs, irrespective of the particular aggregating species, suggesting that recruitment of autophagocytic machinery to sites of IB formation may be a general feature of the cellular defense against protein aggregation (36).

Aggregated proteins in the mammalian cytoplasm are sequestered into pericentriolar IB called "aggresomes" (37). Aggresomes form when

* This work was supported by grants from the National Institutes of Health NS-042842 and the Huntington's Disease Society of America (to R. R. K.). The costs of publication of this article were defrayed in part by the payment of page charges. This article must therefore be hereby marked "*advertisement*" in accordance with 18 U.S.C. Section 1734 solely to indicate this fact.

[S] The on-line version of this article (available at http://www.jbc.org) contains supplemental Figs. S1 and S2.

[1] Present address: Elan Pharmaceuticals, 1000 Gateway Blvd., South San Francisco, CA 94080.

[2] To whom correspondence should be addressed. Tel.: 650-723-7581; Fax: 650-724-4927; E-mail: kopito@stanford.edu.

[3] The abbreviations used are: IB, intracellular inclusion body; HD, Huntington disease; mTOR, mammalian target of rapamycin; RNAi, RNA interference; CFTR, cystic fibrosis transmembrane receptor; GFP, green fluorescent protein; CFP, cyan fluorescent protein; ALLN, *N*-acetyl-Leu-Leu-norleucinal; shRNA, short hairpin RNA.

the ubiquitin proteasome system is overwhelmed with aggregation-prone protein by a process in which small protein aggregates are actively transported on microtubules by a process requiring dynein/dynactin motors (38) and the tubulin deacetylase HDAC6 (39). The recent demonstration that neurons expressing polyglutamine-expanded Htt survive better if they can form aggresomes (18), together with the finding that polyglutamine toxicity is enhanced by microtubule disrupting agents that prevent aggresome formation (40, 41), strongly supports the hypothesis that aggresome formation is a cytoprotective mechanism.

One way that aggresome formation could be cytoprotective would be to facilitate the delivery of dispersed protein aggregates to the autophagy pathway (38). Indeed evidence for such a mechanism is suggested by the demonstration that pharmacological inhibition of autophagy slows the clearance of aggresomes composed of mutant peripheral myelin protein PMP22, a Schwann cell protein associated with a host of demyelinating neuropathies (42).

Autophagy has been primarily considered to be a bulk, non-selective pathway by which cells scavenge cytoplasmic proteins and organelles in response to nutrient deprivation (43). However, efficient degradation of protein aggregates by autophagy requires that they be concentrated in nascent autophagic structures. Previous investigators have reported that microtubule disruption interferes with autophagy by impairing autolysosome formation (44, 45).

Here we show that autophagosome formation is strongly activated by acute proteasome impairment. Because proteasome impairment inevitably accompanies the production and/or accumulation of aggregated proteins (46, 47), this finding suggests a mechanism by which protein aggregation could induce an autophagic response. We find that recruitment of Atgs, aggregates, and lysosomes to aggresomes requires both an intact microtubule cytoskeleton and the tubulin deacetylase, HDAC6. These data suggest that minus-end-directed transport on microtubules is a mechanism used by cells to enhance the efficiency and selectivity of autophagic degradation of aggregated proteins. Thus, the aggresome and autophagy pathways operate cooperatively to eliminate aggregation-prone proteins that escape surveillance by the ubiquitin proteasome system.

MATERIALS AND METHODS

Cell Lines Cell Culture and Transfection—Human embryonic kidney HEK-293 cells, HeLa cells, and neuro2a (N2Aa) cells were cultured in Dulbecco's modified Eagle's medium supplemented with 10% fetal bovine serum and antibiotics at 37 °C in 95 and 5% CO_2. Plasmid transfection was done using Lipofectamine 2000 (Invitrogen) following the manufacturer's protocol. Most of the analyses were done after 48 h of transfection unless otherwise noted. For immunoblotting, cells were lysed in 50 mM Tris, pH 7.5, 100 mM NaCl, 0.5% Triton X-100, 2.5 mM $MgCl_2$ containing 1× protease inhibitors (Roche Applied Science) and phosphatase inhibitors. Extracts were passaged ten times with a 21-gauge needle followed by passage through a 25-gauge needle four times. Extracts were centrifuged at 14,000 rpm for 10 min at 4 °C, and supernatants were quantified using Bio-Rad protein assay (Bio-Rad). Protein was electrophoresed through 18% Tris-glycine gels for LC3-CFP and transferred to polyvinylidene difluoride (Bio-Rad). Membranes were probed overnight at 4 °C with antibody. Protein was visualized with enhanced chemiluminescence (ECL) plus (Amersham Biosciences) and quantified using the Typhoon Imager (Amersham Biosciences) and ImageQuaNT software.

Clonal cell lines were selected and maintained at 800 μg/ml G418 (Invitrogen). The Neuro2a huntingtin-inducible cell line was a generous gift from Dr. Nobuyuki Nukina (Wako-shi, Saitama, Japan) (48).

Plasmid Constructs—CFTR (37) and GFP-Q25 and GFP-Q103 (13) huntingtin constructs were described elsewhere. Human Atg8/LC3 cDNAs were previously described (36).

Antibodies and Reagents—Anti-Atg8/LC3B antibody was generated against full length recombinant human 6His-LC3-I produced in *E. Coli* or N terminus 15 peptides from human LC3B sequence. Anti-HDAC6 antibody was purchased from Calbiochem (La Jolla, CA). Anti-GFP antibody was purchased from Roche (Mannheim, Germany). Anti-actin and anti-ubiquitin monoclonal antibodies were from Chemicon International (Temecula, CA). Anti-myc 9E10 antibody was purchased from Invitrogen. γ-Tubulin antibody was from Sigma. Antibodies to LAMP-1 and LAMP-2 (H4B4) and a-tubulin (DM1a) were obtained from the University of Iowa Hybridoma Bank. Tubacin and niltubacin were a gift from S. Schreiber and J. Bradner (49).

Microscopy—Cells were grown on glass coverslips coated with poly-L-lysine and collagen, fixed in 4% paraformaldehyde, permeabilized by 0.25%Triton X-100, and blocked with 5% bovine serum albumin in phosphate-buffered saline. Primary antibody incubation was done at 4 °C for overnight followed by 1-h incubation at room temperature with Alexa 488 or 546 labeled secondary antibodies (Molecular Probes, Eugene, OR) and 50 μg/ml bisbenzimide (Sigma) for nuclear staining. Conventional epifluorescence micrographs were obtained on a Zeiss Axiovert 200M microscope with a 100× oil lens (NA1.4, Zeiss). Digital (12-bit) images were acquired with a cooled charge-coupled device (Roper Scientific, Trenton, NJ) and processed by using Metamorph software (Universal Imaging, Media, PA). The excitation filters used for conventional microscopy were 365WB50 (bisbenzimide), 440AF21 (CFP), 500AF25 (GFP, Alexa488), and 560AF55 (Alexa546). Emission filters were 450DF65 (bisbenzimide), 480AF30 (CFP), 545AF35 (GFP, alexa488), and 645DF55 (Alexa546). The dichroics were: 400DCLP (bisbenzimide), 455DRLP (CFP), 525DRLP (GFP, Alexa488), and 595DRLP (Alexa546). Confocal images were obtained using a Leica LSM 510 with a 63× oil lens (numerical aperture 1.2, Leica).

Transmission Electron Microscopy—Cells were gently scraped, pelleted, and fixed in 3% paraformaldehyde, 1.5% glutaraldehyde, and 5% sucrose in 0.1 M sodium cacodylate buffer for 3 h at room temperature. Cells were washed briefly in 0.1 M cacodylate buffer, pH 7.4, and post-fixed using 1% osmium tetroxide and 0.5% potassium ferrocyanide in 0.1 M sodium cacodylate buffer for 1 h at room temperature. The cells were washed with 0.05 M cacodylate buffer, *en bloc* stained with 1% uranyl acetate in 10% ethanol for 1 h and rapidly dehydrated through a series of graded ethanol followed by propylene oxide. The cells were placed in a 1:1 mixture of propylene oxide and LX-112 resin (Ladd Research Industries, Williston, VT) overnight, immersed in two changes of LX-112 resin (2 h each), and polymerized at 60 °C for 24–48 h. 60-nm ultrathin sections were contrasted with 2% uranyl acetate for 10 min at room temperature, followed by lead citrate for 2 min at room temperature. Grids were viewed and photographed using a JEOL 1200EX II transmission electron microscope (JEOL, Peabody, MA).

RNA Interference—For HDAC6 knock-down, sequence from 117–136 bp of its open reading frame was subcloned to pSUPER vector (Oligoengine, Seattle, WA).

Filter Trap Assay—A polyglutamine filter trap assay was done following the published protocol (3, 50) using anti-GFP. The protein amount was normalized to equal the amount of soluble fraction.

Promoter Shutdown Experiment—Neuro2a huntingtin-inducible cells, expressing GFP-Htt Q150 under control of an ecdysone promoter (48) were induced with 1 μM ponasterone A for 72 h after which the medium was replaced with Dulbecco's modified Eagle's medium lacking ponasterone A. 5 mM dibutyryl cAMP (N^6,2′-*O*-dibutyryladenosine-

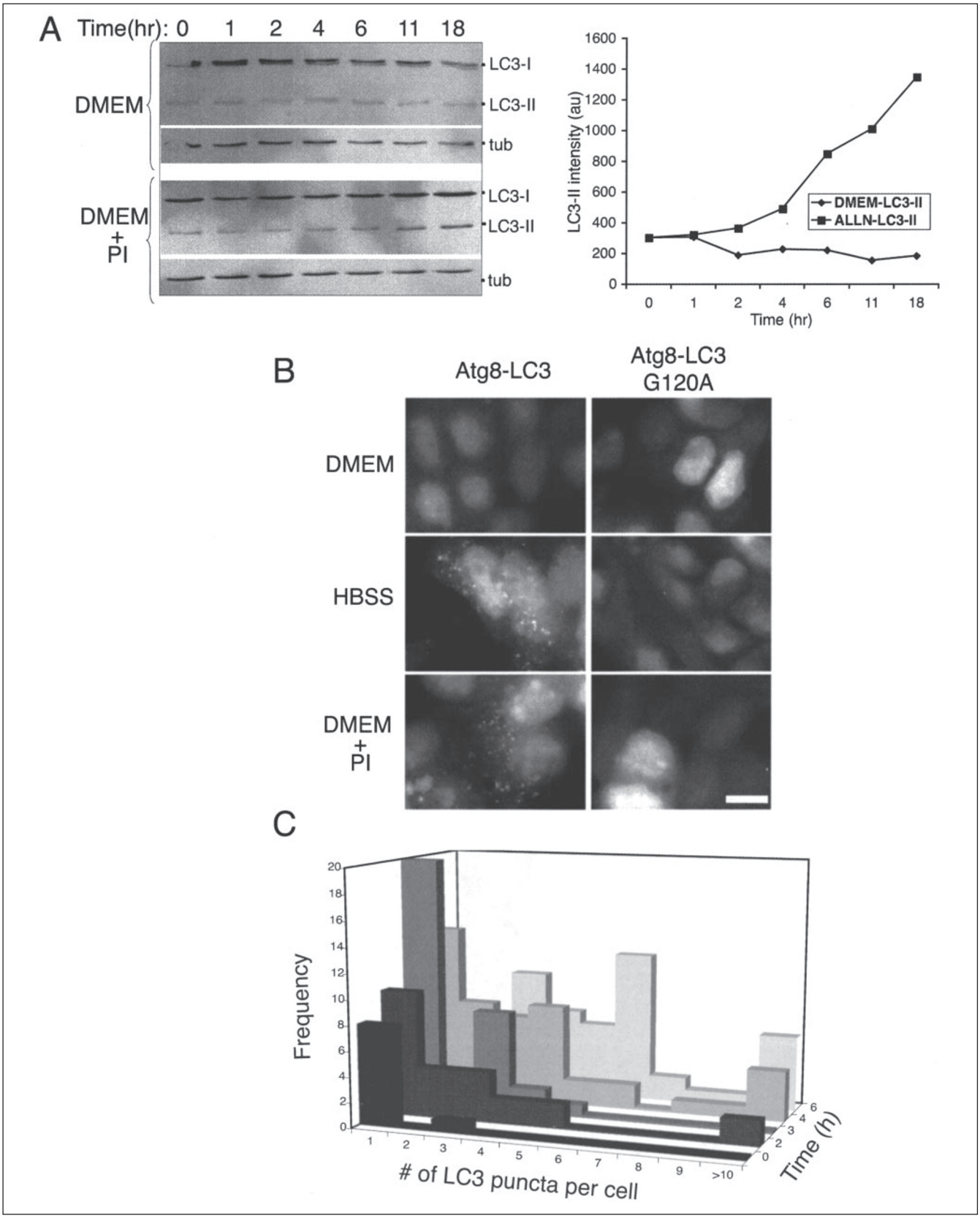

FIGURE 1. **Autophagy is induced by proteasome inhibition.** *A*, time course of Atg8/LC3-II accumulation in cells exposed to proteasome inhibitor. HEK-293 cells stably expressing CFP-LC3 were treated with proteasome inhibitor (*PI*; 10 μg/ml ALLN) for the times indicated, and Atg8/LC3 expression was analyzed by immunoblot analysis (*left panel*) with antibodies to GFP or tubulin as a loading control. LC3-II band intensity was quantified by image analysis and plotted against time (*right panel*); similar profiles were observed for the ratio LC3-II:LC3-I (not shown). *B*, effect of starvation (Hanks' balanced salt solution (*HBSS*) or proteasome inhibition (*PI*; MG132, 25 μM)) on the formation of autophagosomes. HEK-293 cells stably expressing CFP-Atg8/LC3 (*left*) or the inactive mutant CFP-Atg8/LC3G120A cells (*right*) were subjected to the indicated treatments for 3 h and imaged for CFP by autofluorescence microscopy. *Bar* = 2 μm. *C*, time course of LC3-II accumulation in cells monitored by puncta formation using immunofluorescence. Cells were treated with ALLN (10

3′,5′-cyclic monophosphate sodium salt, Sigma) was present throughout the experiment.

Transcription Analysis—Cells were preincubated with methionine, cysteine-free medium for 30 min, then incubated with 10 mCi of [^{35}S]methionine (MP Biomedicals, Irvine, CA). The cells were incubated for 15 min and harvested in phosphate-buffered saline supplemented with 2 mM methionine. Then the cells were lysed and immunoprecipitated by anti-GFP antibody. The amount of protein synthesized during the chase period was analyzed by SDS-PAGE and autoradiography.

Data Analysis—Image analysis was done by Image J version 1.30 (National Institutes of Health). Statistical analyses were done by Statview version 5.0 (SAS institute, Cary, NC) using Student's *t* test. ImageJ Plug-ins Analyze particles and cell counter were used to quantify "autophagosomes" as defined by a threshold value of 159–254 and a particle size of 5.

RESULTS

Proteasome Inhibition Induces Autophagy—In yeast and mammalian cells, autophagy is under strict metabolic control, sensing nutrient insufficiency via the inhibitory TOR (mTOR) signaling pathway, and non-selectively breaking down cellular proteins in response to nutrient availability (25, 51). To test whether autophagy is also activated by intracellular protein aggregation, steady-state levels of the lipid-conjugated form of Atg8/LC3, LC3-II, an established indicator of autophagic activation (52), were assessed in cells exposed to the proteasome inhibitor ALLN (Fig. 1). LC3-II levels increased with time following a 1–2 h lag, in response to exposure to ALLN (Fig. 1*A*) or other proteasome inhibitors (data not shown). Similarly, CFP-LC3-II levels increased in response to proteasome inhibition in cells stably expressing a CFP-tagged form of LC3 (data not shown). The increase in Atg8/LC3-II levels corresponded to the appearance of fluorescent puncta in HEK-293 cells stably expressing CFP-Atg8/LC3 treated with the proteasome inhibitors MG132 (Fig. 1*B*, *bottom panel*), ALLN or lactacystin (data not shown), that were indistinguishable in appearance from autophagosomes formed in response to the classic inducer of macroautophagy: amino acid starvation (Fig. 1*B*, *middle panel*). Similar punctate structures were observed in untransfected HEK-293 cells labeled with antibodies to endogenous Atg8/LC3 and Atg12 (data not shown; see Fig. 2) but not in cells expressing CFP-Atg8/LC3G120A, a conjugation-defective Atg8/LC3 mutant (Fig. 1*B*, *right panels*). Quantification of LC3 puncta formation in HEK-293 cells exposed to ALLN (Fig. 1*C*), revealed that, at rest, the vast majority of cells had ≤1 LC3-positive puncta, whereas the number of cells with multiple puncta increased by 2 h after administration of the drug. Atg8/LC3 remained soluble following extraction of MG132-treated cells with non-ionic detergent and did not appear to form covalent conjugates with ubiquitin (supplemental Fig. S1). These data demonstrate that autophagy is rapidly induced in response to impaired proteasome activity.

Clearance of Protein Aggregates Requires Microtubule-dependent Transport—To assess how proteasome inhibition influences the subcellular distribution of autophagosomes, endogenous Atg8/LC3 was localized in HeLa cells by immunofluorescence microscopy and transmission electron microscopy (Fig. 2). In unperturbed cells (Fig. 2*A*, *panels a–c*), Atg8/LC3 was present in numerous very fine cytoplasmic puncta that were slightly enriched in the Golgi region. In amino acid-starved cells (Fig. 2*A*, *panels d–f*), Atg8/LC3 antibody labeled discrete autophagic structures that were distributed randomly throughout the cytoplasm. No correlation was observed between the distribution of Atg8/LC3 and that of ubiquitin, which maintained a uniformly diffuse distribution in both resting and starved cells. By contrast, overnight exposure to lactacystin (Fig. 2*A*; g-i) or other proteasome inhibitors (data not shown) resulted in a dramatic redistribution of both ubiquitin and Atg8/LC3 immunoreactivity to a discrete juxtanuclear region, where the two antigens appeared to be extensively colocalized. Juxtanuclear concentration and colocalization of ubiquitin and Atg8/LC3 immunoreactive structures was abrogated by treatment with nocodazole (Fig. 2*A*, *panels j–l*). The appearance of LC3-immunopositive puncta in response to proteasome inhibition correlated with the appearance, by transmission electron microscopy (Fig. 2*B*), of multilamellar, darkly stained structures that could be identified as degradative autophagosomes by the presence of membrane-enclosed organelles filled with smaller, electron-dense fragments of cellular debris (Fig. 2*B*, *panel c*). Some of these structures had clear bilamellar or multilamellar morphology characteristic of autophagosomes. Note that autophagic structures are frequently clustered within invaginations of the nuclear envelope (Fig. 2*B*, *panel c*), reminiscent of aggresomes. To confirm an association between aggresomes and autophagosomes, we used transmission electron microscopy to examine autophagosome formation and localization in cells expressing a classic aggresomal substrate, the ΔF508 mutant of the cystic fibrosis transmembrane conductance regulator, CFTR (37) (Fig. 2*C*). *Panel a* shows a typical electron-dense aggresome composed of membrane-free aggregated CFTR protein, completely surrounding a pair of centrioles (*c*), shown at higher magnification in Fig. 2*C* (*panel b*). As seen in untransfected proteasome-inhibited cells (Fig. 2*B*), structures resembling degradative autophagosomes (*AVd*, *asterisks* in Fig. 2*C*, *panel c*) surrounded the aggresome and were clustered between the aggresome and the nuclear envelope. One such structure is shown in more detail in *panel d*. This relationship to the microtubule-organizing center was confirmed by immunofluorescence microscopy (Fig. 3*A*). The site to which autophagosomes and ubiquitinated conjugates clustered was immunoreactive with antibody to γ-tubulin, a centrosomal protein (Fig. 3*A*); nocodazole treatment increased the average distance between centrosomes and Atg-labeled structures (Fig. 3*B*). Therefore, upon proteasome inhibition, delivery of autophagosomes and ubiquitinated proteins to the microtubule organizing center requires an intact microtubule cytoskeleton.

We (36) and others (27, 30, 31) have recently reported that autophagy contributes to the elimination of aggregated proteins containing expanded polyglutamine tracts. Because both aggregated protein and Atg8/LC3 are recruited to the microtubule organizing center, we sought to evaluate the role of microtubules in autophagic degradation of aggregated huntingtin (Fig. 3). We used a promoter shut-off strategy (36) in neuronally differentiated neuro2a cells stably transfected with GFP-HttQ150 under the control of an ecdysone promoter (48). Following induction for 3 days, the inducer was withdrawn, resulting in high level expression of GFP-HttQ150 aggregates, as assessed by filter-trap assays (3, 50) (data not shown) and inclusion body counting (Fig. 3). We have previously established that 1) following induction, the vast majority of Htt is aggregated and 2) the clearance of Htt from these cells following promoter shut-off

μg/ml) for $t = 0$, 1, 2, 3, 4, and 6 h and imaged for CFP fluorescence by confocal microscopy. Each of the five histograms shows the number of cells out of 200 (frequency, *y*-axis) that contained the indicated number of autophagosomes (bins on *x*-axis) at each time point (*z*-axis). The number of cells that contained zero autophagosomes at each time point (not plotted because of scaling incompatibility) was; *t0* = 191, *t2* = 176, *t3* = 166, *t4* = 153, and *t6* = 146.

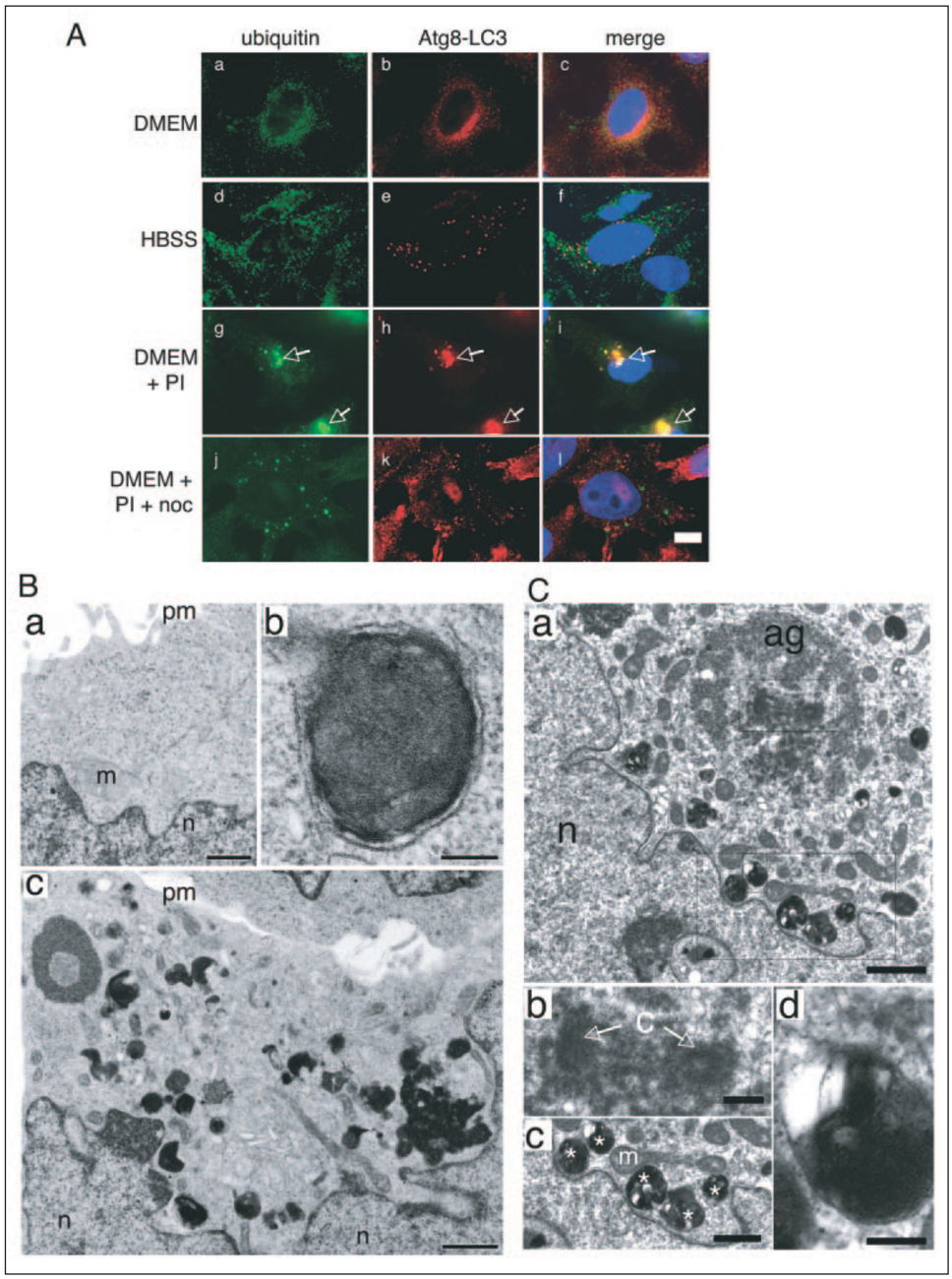

FIGURE 2. **Accumulation of autophagic vacuoles around aggresomes.** *A*, HeLa cells were cultured in Dulbecco's modified Eagle's medium (*a–c*), Hanks' balanced salt solution (*HBSS*) for 4 h (*d–f*), Dulbecco's modified Eagle's medium plus lactacystin (10 μM) for 18 h (*g–i*) or Dulbecco's modified Eagle's medium plus lactacystin (10 μM) with 1 μg/ml nocodazole for 18 h (*j–l*). Cells were fixed and stained with anti-ubiquitin (*a*, *d*, *g*, and *j*) and Atg8/LC3 antibodies (*b*, *e*, *h*, and *k*). *Arrows* indicate aggresomes. *Bar* = 2 μm. *B*, transmission electron microscopy of HEK-293 cells exposed to ALLN for 0 h (*a*), 3 h (*b*), or 21 h (*c*). Typical autophagic structures were absent from untreated cells (*a*) and clearly evident in ALLN-treated cells (*b* and *c*) and increased in abundance with time of exposure to the drug. Note clustering of electron-dense autophagic bodies at juxtanuclear sites (*lower right* of *panel c*). *C*, accumulation of autophagosomes near pericentriolar aggresome. *a*, electron micrograph of HEK-293 cells, transiently expressing the ΔF508 mutant of CFTR, were treated overnight with ALLN. *Boxes* denote regions shown at higher magnification in *panels b–d*. *b*, higher magnification micrograph showing pair of centrioles in the center of the electron dense ΔF508-CFTR aggresome. *c*, *asterisks* denote late degradative autophagosomes. *d*, high magnification view of autophagosome from *panel c*. *Scale bars*, 1 μm. Abbreviations: *ag*, aggresome; *c*, centriole; *n*, nucleus; *m*, mitochondrion; and *pm*, plasma membrane.

is abrogated by RNA silencing of either Atg8/LC3 or Atg12, strongly supporting the conclusion that clearance of aggregated Htt by these cells is strictly dependent on autophagy (36). In the experiment shown in Fig. 3*C*, GFP-HttQ150 aggregates declined by ~40% over the subsequent 4 days. By contrast, exposure to nocodazole led to an increase in aggregate levels by nearly 40% over the same period. Thus, autophagic clearance of aggregated GFP-HttQ150 requires an intact microtubule cytoskeleton.

HDAC6 Is Required for Aggregate Clearance—Recently Kawaguchi *et al.* (39) reported that the cytoplasmic deacetylase HDAC6 is recruited to aggresomes and is required for the dynein-dependent transport of ubiquitinated aggregates to these pericentriolar cytoplasmic inclusion bodies. We observed that GFP-positive cytoplasmic inclusion bodies in HeLa cells expressing GFP-Q103-Htt were prominently labeled by HDAC6 antibody (Fig. 4*A*), indicating that endogenous HDAC6 is recruited to cytoplasmic Htt inclusion bodies. To directly assess the functional role of HDAC6 in the clearance of aggregated Htt, the frequency of detectable IB was monitored in neuro2a cells following promoter shut-off in the presence or absence of RNAi to HDAC6 (Fig. 4*B*). After 3 days of induction of GFP-Htt Q150 expression 29 ± 3.6% of the cells exposed to HDAC6 siRNA had detectable IB, compared with only 18 ± 4.8% of cells exposed to control siRNA vector indicating that Htt Q150 was being actively eliminated by an HDAC6-dependent process during the induction period. The decrease in IB frequency following GFP-Htt Q150 shut-off was completely abrogated by HDAC6 knockdown (Fig. 4*B*) and the level of aggregated Htt Q150, assessed by filter retardation (Fig. 4*C*), was correspondingly increased in HDAC6-deficient cells. These data strongly suggest a role for HDAC6 in autophagic clearance of aggregated Htt.

In addition to its established function in facilitating the transport of aggregated, ubiquitinated proteins to aggresomes (39), HDAC6 could also mediate retrograde transport of components of the autophagy

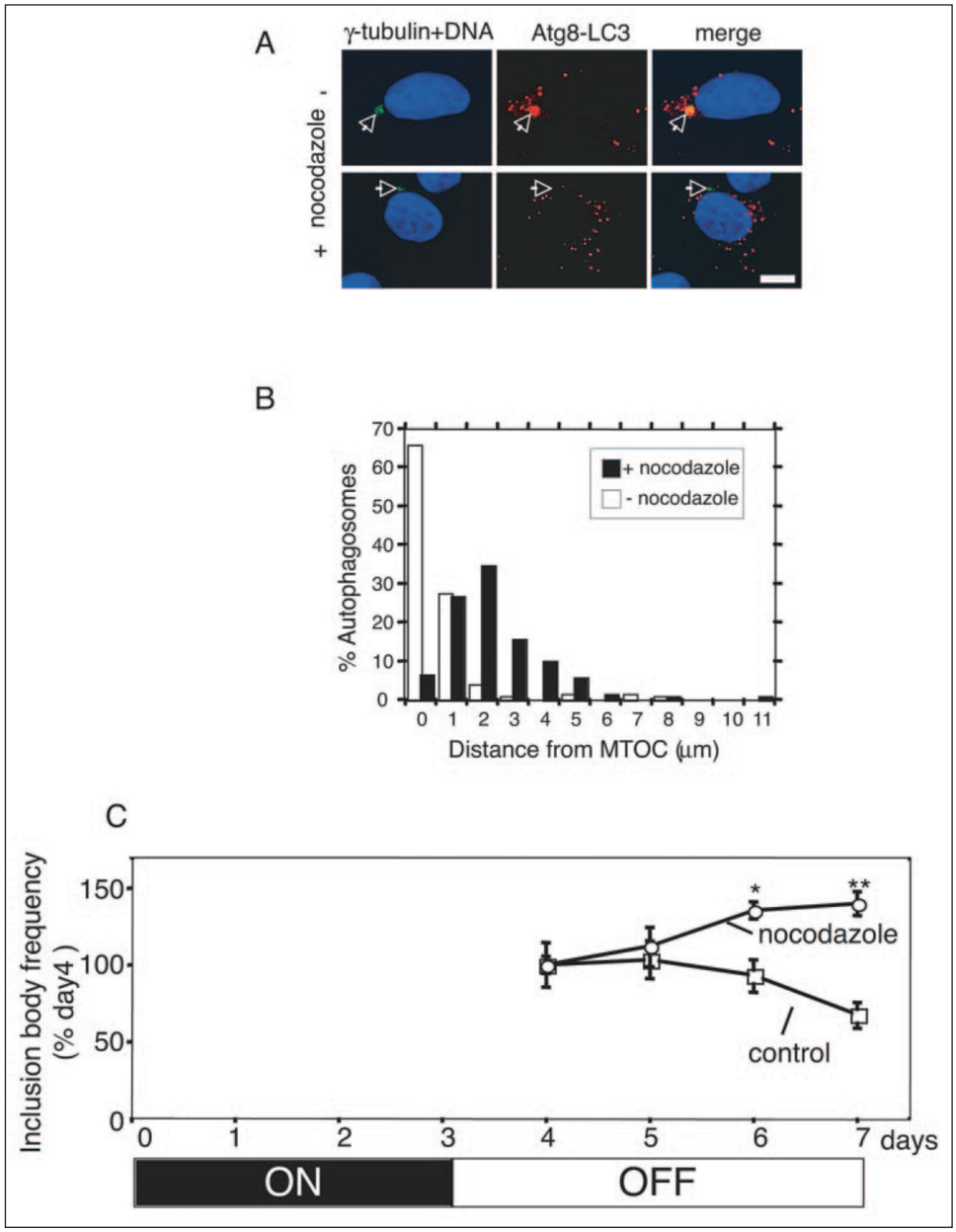

FIGURE 3. **Microtubules are required for LC3 recruitment to aggresomes and for Htt aggregate clearance.** *A*, HeLa cells incubated with 10 μg/ml ALLN for 18 h with or without 1 μg/ml nocodazole were stained with γ-tubulin and Atg8/LC3 antibodies. *Arrows* indicate centrosome. *Bar*, 2 μm. *B*, histogram of distance between centrosome (γ-tubulin staining; *arrows* as in Fig. 2*A*) and Atg8/LC3 immunoreactive puncta in cells incubated in the presence (*black bars*) or absence (*white bars*) of nocodazole. Data are represented as a percentage of 150–200 individual Atg8/LC3-positive puncta from five randomly selected cells in each condition. *C*, microtubules are required for clearance of huntingtin aggregates. Neuro2a cells expressing GFP-Htt Q150 were differentiated and induced with ponasterone A for 72 h ("*ON*") followed by incubation in the presence or absence of nocodazole (0.1 μg/ml) for 4 days in medium lacking inducer ("*OFF*"). At indicated times cells were counted and scored for the presence of GFP-positive inclusion bodies. *y*-axis values are the fraction of IB-containing cells at each time point expressed as a percentage of the fraction of IB-containing cells at day 4 (~45% for both conditions). $n = 150$ from 3 independent experiments. *, $p = 0.0251$; **, $p = 0.0033$ *versus* control.

machinery. To test this, we measured the effect of HDAC6 knockdown on recruitment of Atg8/LC3 to GFP-Htt Q103 inclusion bodies (Fig. 4*D*). Although 92 ± 5.8% of IB in cells treated with control RNAi were clearly labeled with Atg8/LC3 antibody, only 43 ± 9.7% of IBs were Atg-positive following HDAC6 knockdown. HDAC6 has been proposed to function as a linker, capable of forming a ternary complex between ubiquitinated proteins and dynein (39). Although this model could explain the requirement for HDAC6 in delivery of aggregated proteins to pericentriolar inclusion bodies, it is not at all clear how such a linker function could mediate the recruitment of components of the autophagy or lysosomal apparatus, because these structures are not likely to be modified with ubiquitin. To clarify the mechanism by which HDAC6 mediates recruitment of LC3 to aggresomes, we took advantage of tubacin, a recently described, highly selective inhibitor of HDAC6 catalytic activity (49). Treatment of Neuro2a cells induced to express GFP-Htt Q150 with tubacin strongly inhibited recruitment of LC3 to GFP-positive foci, whereas treatment with the inactive carboxylate analog, niltubacin, or carrier (Me_2SO) had no effect (Fig. 4*E*, data not shown). The effect of tubacin was reversible, as evidenced by colocalization of LC3 to GFP-positive aggresomes following washout of the drug. These data demonstrate that HDAC6 protein and HDAC6 catalytic function is required for transport of LC3 to the aggresomes.

Autophagic protein degradation requires fusion of autophagosomes with lysosomes to form autolysosomes in which substrates are exposed to the acidic pH and hydrolytic activities to which lysosomes are endowed. Lysosomes are normally concentrated in mammalian cells in a pericentriolar region by a dynamic balance between retrograde and anterograde transport on microtubules (53). Previous studies have reported that microtubule disruption impairs starvation-induced, bulk-phase autophagic protein degradation, leading to the proposal that microtubule-dependent processes may facilitate autolysosome formation (44). Hence, we considered the possibility that HDAC6 may be required for retrograde transport of lysosomes. Lysosomes, labeled with antibody to the lysosomal membrane protein, LAMP2 (Fig. 5*A*) and other endosomal/lysosomal markers including LAMP1, cathepsin D,

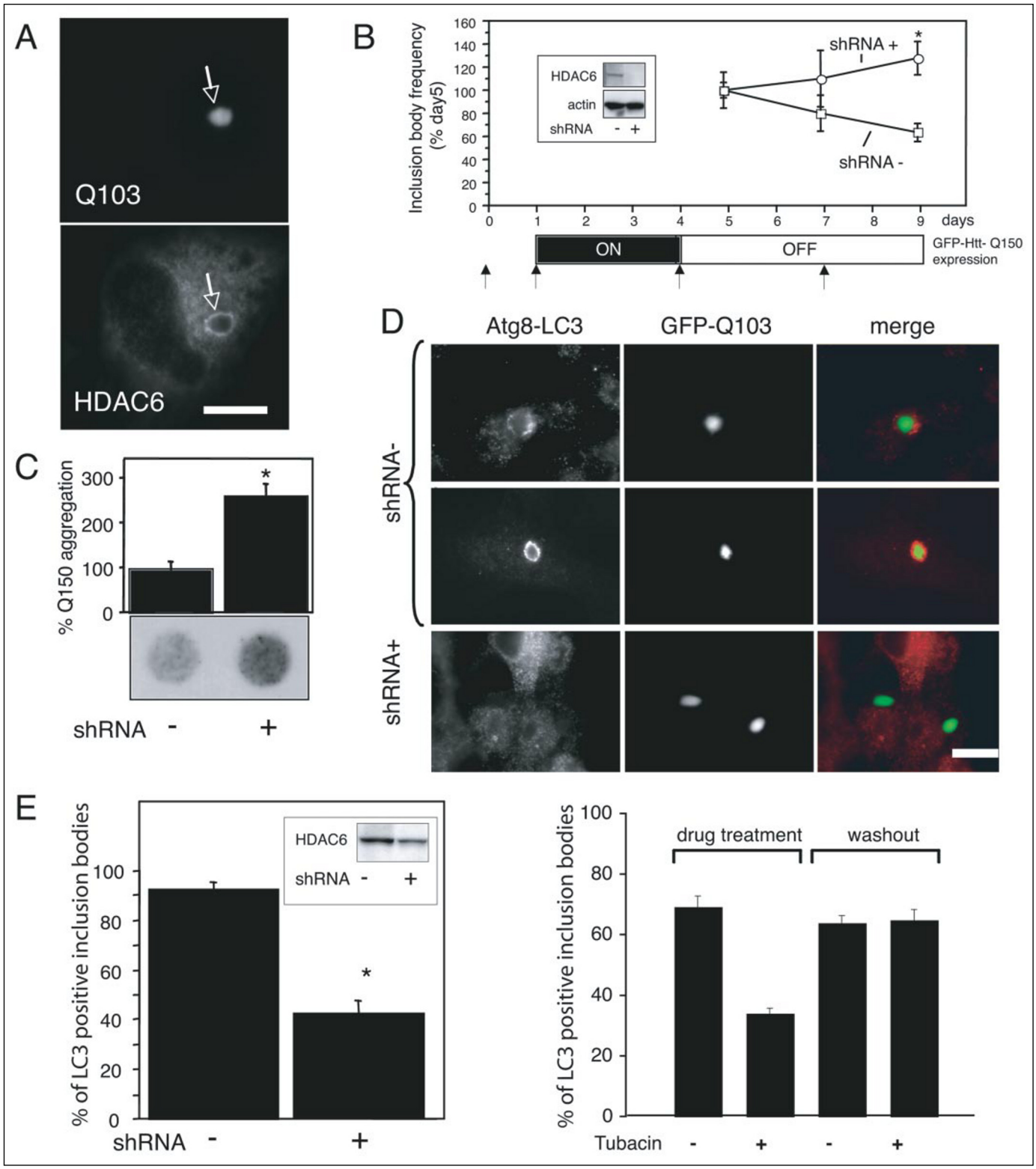

FIGURE 4. **HDAC6 is required for clearance of aggregated Htt.** *A*, HDAC6 colocalizes to Htt Q103 inclusions. HeLa cells transiently expressing GFP-Htt Q103 were imaged for GFP fluorescence or HDAC6 immunofluorescence. *Bar* = 2 μm. *B*, neuro2a cells were induced to express GFP-Htt Q150 for 3 days ("*ON*", timeline, *bottom*) followed by 6 days in culture without inducer ("*OFF*"). Cells were transfected with pSUPER or pSUPER containing shRNA sequence for HDAC6 on day 0. 1, 4, and 7 (*upward arrows*) and scored for the presence of inclusion bodies by microscopy from days 5 to 9. Data are normalized to 100% on day 5 for each condition, to permit comparison of rates. *Inset* shows extent knock-down of HDAC6 on day 5 detected by immunoblot. Actin blot is shown as a loading control. $n = 120$ from 3 independent experiments. *, $p = 0.0052$ *versus* shRNA. *C*, effect of HDAC6 knockdown on GFP-Htt Q150 aggregation. Filter retardation assay was performed on lysates of neuro2a cells transfected with pSUPER vector alone (−) or with pSUPER containing shRNA (+) 5 days following removal of inducer. *, $p = 0.0364$ *versus* shRNA−. D/E. HDAC6 knockdown affects Atg8/LC3 colocalization with GFP-Htt inclusions in HeLa cells. *Inset* shows extent of HDAC6 knockdown. *, $p = 0.0001$ *versus* shRNA−. *F*, the domain-selective small-molecule inhibitor, tubacin affects colocalization of Atg8/LC3 with GFP-htt-Q15 inclusions in Neuro2a cells. Neuro2a cells were induced to express GFP-Htt Q150 for 3 days ("*ON*"), followed by 2 days in culture without inducer ("*OFF*"). Cells were then treated with tubacin (2 mM, +) or carrier (Me_2SO, −) for 5 h (drug treatment). Treatment with drug, the cells were washed extensively after which fresh media was added without drug for 18 h (washout). *, $p < 0.005$ for drug treatment (+ *versus* −).

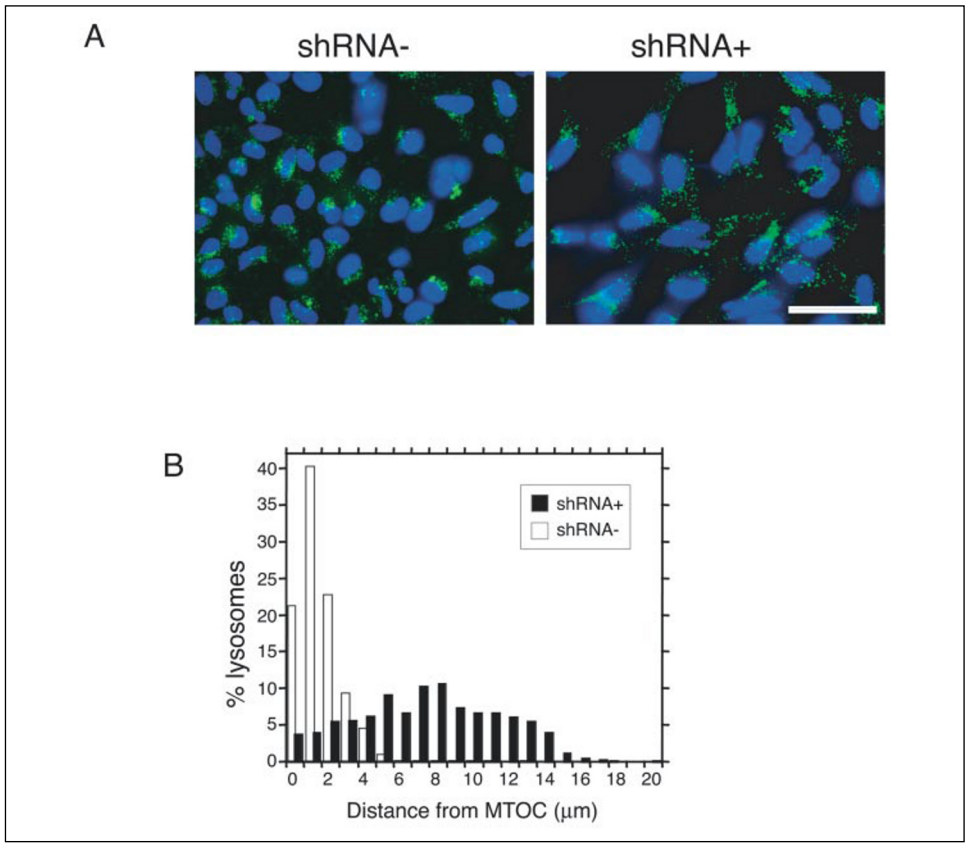

FIGURE 5. **HDAC6 is required for lysosome enrichment around microtubule organizing center.** HeLa cells transfected with pSUPER vector alone (shRNA−) or with pSUPER containing shRNA (shRNA+) for HDAC6 were stained with LAMP-2 antibody. *Bar* = 10 μm. *B*, histogram showing distances between the centrosome (γ-tubulin) and lysosomes (LAMP-2) from cells expressing control shRNA (*white bars*) and HDAC6 shRNA (*black bars*). *n* = 600–1200 spots from 6 randomly selected cells for each condition.

rab7, and rab9 (data not shown) were distinctly enriched at one side of the nucleus of unperturbed HeLa cells, consistent with their concentration to the microtubule organizing center (53). By contrast, lysosomes in cells exposed to HDAC6 RNAi were more randomly distributed. The dispersion of lysosomes upon HDAC6 relative to the centrosome, marked by staining with γ-tubulin antibody (Fig. 5*B*), was quantified by measuring the distance between individual LAMP2- and γ-tubulin-labeled puncta from images such as those shown in Fig. 5*A*, but at higher magnification. Whereas, in control cells, lysosomes were 1.97 ± 0.05 μm from the centrosome, in HDAC knockdown cells the mean distance was increased to 7.87 ± 0.10 μm. These data demonstrate that HDAC6 is required to maintain a pericentriolar position of lysosomes.

DISCUSSION

Protein aggregation is tightly linked to cell dysfunction and death in neurodegenerative disease. Several recent studies suggest a role for autophagy in the clearance of aggregated proteins. It has remained unclear, however, how these aggregates are efficiently collected and delivered to autophagosomes, particularly in light of the view that autophagy is a bulk cytosolic degradation process evolved to generate amino acids during periods of nutrient deprivation. The data reported here establish a role for HDAC6 and the microtubule cytoskeleton in autophagic degradation of protein aggregates and suggest that efficient autophagic degradation requires delivery of the autophagic machinery and substrates to a central, pericentriolar location.

Although autophagy is widely considered to be non-selective, there is evidence that damaged organelles, including mitochondria (54) and peroxisomes (55), are selectively captured by autophagy and degraded in lysosomes. Moreover, the cytoplasm-to-vacuole (*cvt*) pathway, which shares extensive genetic, and hence, mechanistic overlap with the autophagy pathway, delivers the vacuolar hydrolases aminopeptidase I (25) and α-mannosidase (56) to yeast vacuoles, thereby demonstrating that non-selectivity is not an obligatory feature of autophagy. Our data suggest a model for autophagic capture of aggregated protein in which microtubule-dependent retrograde transport provides a means for concentrating substrate and hence, provides a measure of selectivity in aggregate clearance (Fig. 6). In the absence of any specific autophagic targeting signal, autophagic capture of aggregates that are randomly distributed within the cytoplasm must be inefficient, because the concentration of aggregate within the nascent autophagic vesicle cannot be higher than in the surrounding cytoplasm (Fig. 6*A*). This mode may suffice for starvation-induced autophagy, where the goal is to breakdown cytosolic constituents non-selectively to provide amino acids for the maintenance of essential cellular functions. Indeed, earlier studies have established that ribosomes and other cytoplasmic constituents are present within autophagosomes at the same concentrations as in the surrounding cytosol (57). Consistent with this view we find that autophagic structures, marked by Atg8/LC3 (Fig. 1), are distributed randomly throughout the cytoplasm of amino acid-starved cells. However, protein aggregates are concentrated at pericentriolar sites called aggresomes via dynein-dependent transport (38). Our data reveal that Atg8/LC3 is also recruited to aggresomes by microtubule-dependent retrograde transport. Thus, delivery of both the autophagic machinery (Atg8/LC3) and the substrate (aggregated, ubiquitinated protein) to the same restricted cellular space provides a *de facto* mechanism of selectivity for an otherwise non-selective pathway (Fig. 6*B*). It is unlikely that Atg8-LC3 is recruited to IB, because it is itself aggregated under the conditions used in our experiments, because pulse-chase studies reveal it to be very stable ($t_{½} > 12$ h) and unaffected by proteasome inhibition (supplemental Fig. S1). It is well established that lysosomes and recycling endosomes are enriched in the juxtanuclear region by an active

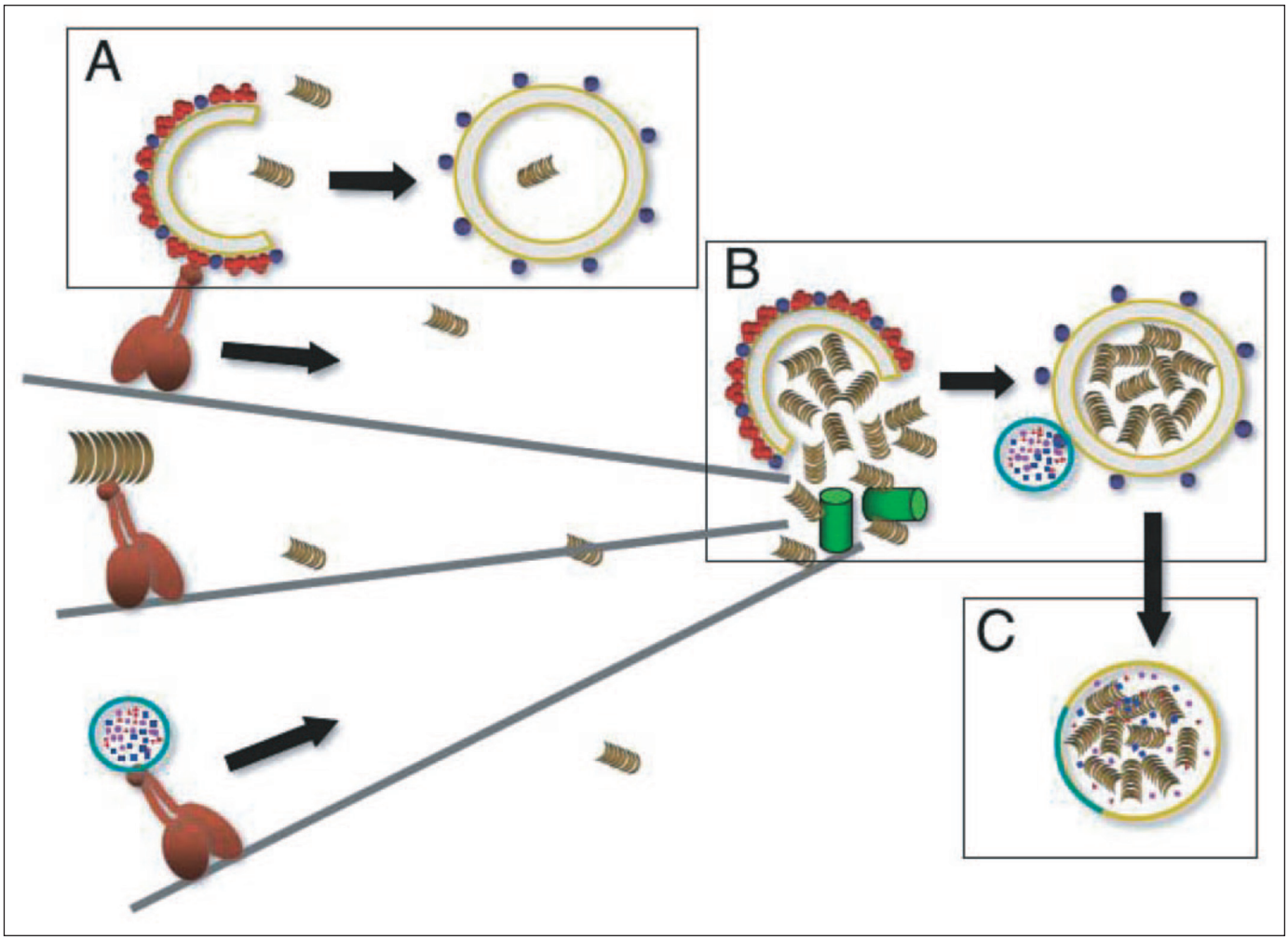

FIGURE 6. **Model for microtubule-dependent recruitment of autophagic machinery.** *A*, bulk autophagy. Isolation membrane ("*C*"-shaped structure) decorated with Atg5–12-16L complex (*red triad*) and Atg8/LC3 (*blue circles*) captures protein aggregates (*gold*) non-selectively and inefficiently. Note Atg5–12-16L complex dissociates upon formation of double-membrane autophagosome. *B*, effect of retrograde transport of aggregate (substrate), autophagic precursors, and endosomes/lysosomes (*green circles*) to pericentriolar region enhances efficiency of capture and autolysosome formation (*C*).

process requiring an intact microtubule cytoskeleton (53) and dynein/dynactin (58). It is thus also probable that assembly of autophagosomes in this region enhances the efficiency of autolysosome formation (Fig. 6*C*).

Recently, an essential role for the cytoplasmic deacetylase, HDAC6, in the microtubule- and dynein-dependent delivery of ubiquitin-conjugated protein aggregates to pericentriolar inclusion bodies, was reported (39). HDAC6 is a multidomain protein that possesses a BUZ-finger domain, which binds to polyubiquitin chains, and two deacetylase domains interrupted by a motif that binds to cytoplasmic dynein (59, 60). Deletion mutagenesis supports a model wherein HDAC can form a ternary complex with aggregates (via ubiquitin association) and with dynein, thereby serving as a linker coupling protein aggregates to the retrograde microtubule motor (39, 61). Curiously, mutations disrupting the deacetylase active site abrogate the function of HDAC6 in this pathway, suggesting an essential role for deacetylation in aggresome formation (39). Our data establish that HDAC6 is essential for retrograde transport of autophagosomes and lysosomes. Because these structures are presumably not conjugated to ubiquitin, how HDAC6 contributes to dynein capture or transport of these organelles remains an interesting but unanswered question. The observation that tubacin, a selective inhibitor of HDAC6 deacetylase activity also blocks LC3 recruitment suggests that deacetylation is essential for this process. It is tempting to speculate that the acetylation state of tubulin, the first substrate of HDAC6 to be described (59), might regulate the nature of interaction of and/or the directionality of microtubule motors. Yet, the influence of other HDAC6 substrates that have been identified (62) or unidentified cannot be excluded. Future studies will be needed to determine how cytoplasmic acetylation regulates organelle transport on microtubules.

Our data suggest that regulation of autophagy is tightly linked to the control of proteasome activity. We find that exposure to proteasome inhibitors leads to increased accumulation of LC3-II, the active form of Atg8/LC3. The mechanism for this up-regulation is unclear at present. The autophagic pathway in mammalian cells is subject to complex regulation by various signaling pathways, including extracellular signal-regulated kinases 1/2, mitogen-activated protein kinases, heterotrimeric G-proteins, mammalian target of rapamycin (mTOR), and its downstream targets p70S6 kinase and eukaryotic translation elongation initiation factor 2 kinase (43). Perhaps, under conditions of nutrient sufficiency, autophagy is activated by proteasome inhibition through homoeostatic stress-response signaling (63) that senses the presence of misfolded proteins or molecular chaperone levels. Indeed, many of the yeast *ATG* genes are activated by heat shock and other classic inducers

of protein stress.[4] A recent study reported that chronic (36–48 h) treatment of neurons with proteasome inhibitors gave rise to increased lysosomes and autophagic structures, suggesting that autophagy could be induced in response to chronic stress (64). Our data extend these findings to establish that autophagy is an acute response to proteasome dysfunction and can become activated within 2 h of proteasome inhibition. Because production and/or accumulation of intracellular protein aggregates impairs proteasome function (13, 14) aggregate accumulation could be a signal that couples activation of autophagy to impairment of the ubiquitin proteasome pathway. Indeed, the recent report that expression of aggregation-prone mutants of α-synuclein, a protein which inhibits proteasome function (65, 66) induces macroautophagy, supports this model.

Mammalian cells are endowed with three levels of defense against the potentially toxic effects of protein aggregates. Molecular chaperones suppress protein misfolding and aggregation, and the ubiquitin-proteasome system degrades misfolded proteins that are unable to fold. Our data suggest that autophagy functions as the third line, eliminating proteins that have escaped the surveillance of the other two systems. Regulation of all three of these systems is highly coordinated, underscoring the importance of aggregation avoidance to organismal survival. Clearly, a deeper understanding of the mechanism by which proteins are targeted for autophagy will aid our understanding of the pathogenesis and facilitate development of rational treatments for conformational diseases.

Acknowledgments—We are indebted to Timo Meerloo, Hyacynth Gacula, and Krystyna Kudlicka (University of California at San Diego) for expert assistance with electron microscopy (Fig. 2B) and to Marilyn G. Farquhar for stimulating discussions and help with ultrastructural analysis. We are grateful to James E. Bradner and Stuart L. Schreiber (Harvard) for the generous gift of tubacin and niltubacin. We thank Nafisa Ghori for help in preparing the sections in Fig. 2C. Finally we thank the members of the Kopito laboratory for insightful discussions of the data.

REFERENCES

1. Zoghbi, H. Y., and Orr, H. T. (2000) *Annu. Rev. Neurosci.* **23,** 217–247
2. Huntington's Disease Collaborative Research Group (1993) *Cell* **72,** 971–983
3. Scherzinger, E., Lurz, R., Turmaine, M., Mangiarini, L., Hollenbach, B., Hasenbank, R., Bates, G. P., Davies, S. W., Lehrach, H., and Wanker, E. E. (1997) *Cell* **90,** 549–558
4. Menalled, L. B., and Chesselet, M. F. (2002) *Trends Pharmacol. Sci.* **23,** 32–39
5. Jackson, G. R., Salecker, I., Dong, X., Yao, X., Arnheim, N., Faber, P. W., MacDonald, M. E., and Zipursky, S. L. (1998) *Neuron* **21,** 633–642
6. Taylor, J. P., Hardy, J., and Fischbeck, K. H. (2002) *Science* **296,** 1991–1995
7. Horwich, A. L., and Weissman, J. S. (1997) *Cell* **89,** 499–510
8. Kopito, R. R., and Ron, D. (2000) *Nat. Cell Biol.* **2,** E207–E209
9. Nucifora, F. C., Jr., Sasaki, M., Peters, M. F., Huang, H., Cooper, J. K., Yamada, M., Takahashi, H., Tsuji, S., Troncoso, J., Dawson, V. L., Dawson, T. M., and Ross, C. A. (2001) *Science* **291,** 2423–2428
10. Steffan, J. S., Kazantsev, A., Spasic-Boskovic, O., Greenwald, M., Zhu, Y. Z., Gohler, H., Wanker, E. E., Bates, G. P., Housman, D. E., and Thompson, L. M. (2000) *Proc. Natl. Acad. Sci. U. S. A.* **97,** 6763–6768
11. Gunawardena, S., Her, L. S., Brusch, R. G., Laymon, R. A., Niesman, I. R., Gordesky-Gold, B., Sintasath, L., Bonini, N. M., and Goldstein, L. S. (2003) *Neuron* **40,** 25–40
12. Hashimoto, M., Rockenstein, E., Crews, L., and Masliah, E. (2003) *Neuromolecular Med.* **4,** 21–36
13. Bence, N., Sampat, R., and Kopito, R. R. (2001) *Science* **292,** 1552–1555
14. Jana, N. R., Zemskov, E. A., Wang, G., and Nukina, N. (2001) *Hum. Mol. Genet.* **10,** 1049–1059
15. Caughey, B., and Lansbury, P. T. (2003) *Annu. Rev. Neurosci.* **26,** 267–298
16. Ross, C. A., and Poirier, M. A. (2004) *Nat. Med.* **10,** S10–S17
17. Bennett, E. J., Bence, N. F., Jayakumar, R., and Kopito, R. R. (2005) *Mol. Cell* **17,** 351–365
18. Arrasate, M., Mitra, S., Schweitzer, E. S., Segal, M. R., and Finkbeiner, S. (2004) *Nature* **431,** 805–810
19. Hazeki, N., Tukamoto, T., Goto, J., and Kanazawa, I. (2000) *Biochem. Biophys. Res. Commun.* **277,** 386–393
20. Davies, S. W., Turmaine, M., Cozens, B. A., DiFiglia, M., Sharp, A. H., Ross, C. A., Scherzinger, E., Wanker, E. E., Mangiarini, L., and Bates, G. P. (1997) *Cell* **90,** 537–548
21. Yamamoto, A., Lucas, J. J., and Hen, R. (2000) *Cell* **101,** 57–66
22. Zu, T., Duvick, L. A., Kaytor, M. D., Berlinger, M. S., Zoghbi, H. Y., Clark, H. B., and Orr, H. T. (2004) *J. Neurosci.* **24,** 8853–8861
23. Mortimore, G. E., Miotto, G., Venerando, R., and Kadowaki, M. (1996) *Subcell Biochem.* **27,** 93–135
24. Klionsky, D. J., Cregg, J. M., Dunn, W. A., Jr., Emr, S. D., Sakai, Y., Sandoval, I. V., Sibirny, A., Subramani, S., Thumm, M., Veenhuis, M., and Ohsumi, Y. (2003) *Dev Cell* **5,** 539–545
25. Klionsky, D. J., and Ohsumi, Y. (1999) *Annu. Rev. Cell Dev. Biol.* **15,** 1–32
26. Petiot, A., Ogier-Denis, E., Blommaart, E. F., Meijer, A. J., and Codogno, P. (2000) *J. Biol. Chem.* **275,** 992–998
27. Ravikumar, B., Stewart, A., Kita, H., Kato, K., Duden, R., and Rubinsztein, D. C. (2003) *Hum. Mol. Genet.* **12,** 985–994
28. Qin, Z. H., Wang, Y., Kegel, K. B., Kazantsev, A., Apostol, B. L., Thompson, L. M., Yoder, J., Aronin, N., and DiFiglia, M. (2003) *Hum. Mol. Genet.* **12,** 3231–3244
29. Hay, N., and Sonenberg, N. (2004) *Genes Dev.* **18,** 1926–1945
30. Ravikumar, B., Duden, R., and Rubinsztein, D. C. (2002) *Hum. Mol. Genet.* **11,** 1107–1117
31. Ravikumar, B., Vacher, C., Berger, Z., Davies, J. E., Luo, S., Oroz, L. G., Scaravilli, F., Easton, D. F., Duden, R., O'Kane, C. J., and Rubinsztein, D. C. (2004) *Nat. Genet.* **36,** 585–595
32. Kegel, K. B., Kim, M., Sapp, E., McIntyre, C., Castano, J. G., Aronin, N., and DiFiglia, M. (2000) *J. Neurosci.* **20,** 7268–7278
33. Sapp, E., Schwarz, C., Chase, K., Bhide, P. G., Young, A. B., Penney, J., Vonsattel, J. P., Aronin, N., and DiFiglia, M. (1997) *Ann. Neurol.* **42,** 604–612
34. Nixon, R. A., Cataldo, A. M., and Mathews, P. M. (2000) *Neurochem. Res.* **25,** 1161–1172
35. Larsen, K. E., and Sulzer, D. (2002) *Histol. Histopathol.* **17,** 897–908
36. Iwata, A., Christianson, J., Bucci, M., Ellerby, L., Nukina, N., Forno, L., and Kopito, R. (2005) *Proc. Natl. Acad. Sci. U. S. A.* **102,** 13135–13140
37. Johnston, J. A., Ward, C. L., and Kopito, R. R. (1998) *J. Cell Biol.* **143,** 1883–1898
38. Kopito, R. R. (2000) *Trends Cell Biol.* **10,** 524–530
39. Kawaguchi, Y., Kovacs, J. J., McLaurin, A., Vance, J. M., Ito, A., and Yao, T. P. (2003) *Cell* **115,** 727–738
40. Muchowski, P. J., Ning, K., D'Souza-Schorey, C., and Fields, S. (2002) *Proc. Natl. Acad. Sci. U. S. A.* **99,** 727–732
41. Taylor, J. P., Tanaka, F., Robitschek, J., Sandoval, C. M., Taye, A., Markovic-Plese, S., and Fischbeck, K. H. (2003) *Hum. Mol. Genet.* **12,** 749–757
42. Fortun, J., Dunn, W. A., Jr., Joy, S., Li, J., and Notterpek, L. (2003) *J. Neurosci.* **23,** 10672–10680
43. Kamada, Y., Sekito, T., and Ohsumi, Y. (2004) *Curr. Top. Microbiol. Immunol.* **279,** 73–84
44. Aplin, A., Jasionowski, T., Tuttle, D. L., Lenk, S. E., and Dunn, W. A., Jr. (1992) *J. Cell. Physiol.* **152,** 458–466
45. Webb, J. L., Ravikumar, B., and Rubinsztein, D. C. (2004) *Int. J. Biochem. Cell Biol.* **36,** 2541–2550
46. Liu, C. W., Giasson, B. I., Lewis, K. A., Lee, V. M., Demartino, G. N., and Thomas, P. J. (2005) *J. Biol. Chem.* **280,** 22670–22678
47. Park, Y., Hong, S., Kim, S. J., and Kang, S. (2005) *Mol. Cells* **19,** 23–30
48. Wang, G. H., Mitsui, K., Kotliarova, S., Yamashita, A., Nagao, Y., Tokuhiro, S., Iwatsubo, T., Kanazawa, I., and Nukina, N. (1999) *Neuroreport* **10,** 2435–2438
49. Haggarty, S. J., Koeller, K. M., Wong, J. C., Grozinger, C. M., and Schreiber, S. L. (2003) *Proc. Natl. Acad. Sci. U. S. A.* **100,** 4389–4394
50. Wanker, E. E., Scherzinger, E., Heiser, V., Sittler, A., Eickhoff, H., and Lehrach, H. (1999) *Methods Enzymol.* **309,** 375–386
51. Yoshimori, T. (2004) *Biochem. Biophys. Res. Commun.* **313,** 453–458
52. Kabeya, Y., Mizushima, N., Ueno, T., Yamamoto, A., Kirisako, T., Noda, T., Kominami, E., Ohsumi, Y., and Yoshimori, T. (2000) *EMBO J.* **19,** 5720–5728
53. Matteoni, R., and Kreis, T. E. (1987) *J. Cell Biol.* **105,** 1253–1265
54. Elmore, S. P., Qian, T., Grissom, S. F., and Lemasters, J. J. (2001) *FASEB J.* **15,** 2286–2287
55. Tuttle, D. L., and Dunn, W. A., Jr. (1995) *J. Cell Sci.* **108,** 25–35
56. Hutchins, M. U., and Klionsky, D. J. (2001) *J. Biol. Chem.* **276,** 20491–20498
57. Kopitz, J., Kisen, G. O., Gordon, P. B., Bohley, P., and Seglen, P. O. (1990) *J. Cell Biol.* **111,** 941–953
58. Burkhardt, J. K., Echeverri, C. J., Nilsson, T., and Vallee, R. B. (1997) *J. Cell Biol.* **139,** 469–484
59. Hubbert, C., Guardiola, A., Shao, R., Kawaguchi, Y., Ito, A., Nixon, A., Yoshida, M., Wang, X. F., and Yao, T. P. (2002) *Nature* **417,** 455–458

[4] R. R. Kopita, unpublished data.

60. Seigneurin-Berny, D., Verdel, A., Curtet, S., Lemercier, C., Garin, J., Rousseaux, S., and Khochbin, S. (2001) *Mol. Cell. Biol.* **21,** 8035–8044
61. Kopito, R. R. (2003) *Mol. Cell* **12,** 1349–1351
62. Kovacs, J. J., Murphy, P. J., Gaillard, S., Zhao, X., Wu, J. T., Nicchitta, C. V., Yoshida, M., Toft, D. O., Pratt, W. B., and Yao, T. P. (2005) *Mol. Cell* **18,** 601–607
63. Ron, D. (2002) *J. Clin. Invest.* **110,** 1383–1388
64. Rideout, H. J., Lang-Rollin, I., and Stefanis, L. (2004) *Int. J. Biochem. Cell Biol.* **36,** 2551–2562
65. Snyder, H., Mensah, K., Theisler, C., Lee, J., Matouschek, A., and Wolozin, B. (2003) *J. Biol. Chem.* **278,** 11753–11759
66. Petrucelli, L., O'Farrell, C., Lockhart, P. J., Baptista, M., Kehoe, K., Vink, L., Choi, P., Wolozin, B., Farrer, M., Hardy, J., and Cookson, M. R. (2002) *Neuron* **36,** 1007–1019